Evidence of Υ(1S)→J/ψ+χ_{c1} and search for double-charmonium production in Υ(1S) and Υ(2S) decays

S. D. Yang *et al.* (Belle Collaboration)

Evidence of $\Upsilon(1S) \to J/\psi + \chi_{c1}$ and search for double-charmonium production in $\Upsilon(1S)$ and $\Upsilon(2S)$ decays

S. D. Yang,[50] C. P. Shen,[2] Y. Ban,[50] A. Abdesselam,[56] I. Adachi,[14, 10] H. Aihara,[60] S. Al Said,[56, 28] K. Arinstein,[4] D. M. Asner,[49] V. Aulchenko,[4] T. Aushev,[23] R. Ayad,[56] A. M. Bakich,[55] V. Bansal,[49] P. Behera,[17] B. Bhuyan,[16] A. Bobrov,[4] A. Bozek,[46] M. Bračko,[35, 24] T. E. Browder,[13] D. Červenkov,[5] V. Chekelian,[36] A. Chen,[43] B. G. Cheon,[12] K. Chilikin,[23] R. Chistov,[23] K. Cho,[29] V. Chobanova,[36] S.-K. Choi,[11] Y. Choi,[54] D. Cinabro,[65] J. Dalseno,[36, 58] M. Danilov,[23, 38] J. Dingfelder,[3] Z. Doležal,[5] Z. Drásal,[5] A. Drutskoy,[23, 38] K. Dutta,[16] S. Eidelman,[4] H. Farhat,[65] J. E. Fast,[49] T. Ferber,[8] V. Gaur,[57] N. Gabyshev,[4] S. Ganguly,[65] A. Garmash,[4] R. Gillard,[65] Y. M. Goh,[12] B. Golob,[33, 24] J. Haba,[14, 10] T. Hara,[14, 10] K. Hayasaka,[41] H. Hayashii,[42] X. H. He,[50] W.-S. Hou,[45] M. Huschle,[26] T. Iijima,[41, 40] K. Inami,[40] A. Ishikawa,[59] R. Itoh,[14, 10] I. Jaegle,[13] D. Joffe,[27] K. K. Joo,[6] T. Julius,[37] T. Kawasaki,[47] D. Y. Kim,[53] H. J. Kim,[31] J. B. Kim,[30] J. H. Kim,[29] K. T. Kim,[30] K. Kinoshita,[7] B. R. Ko,[30] P. Kodyš,[5] S. Korpar,[35, 24] P. Križan,[33, 24] P. Krokovny,[4] A. Kuzmin,[4] Y.-J. Kwon,[67] J. S. Lange,[9] J. Li,[52] Y. Li,[64] L. Li Gioi,[36] J. Libby,[17] D. Liventsev,[14] P. Lukin,[4] K. Miyabayashi,[42] H. Miyata,[47] A. Moll,[36, 58] R. Mussa,[22] E. Nakano,[48] M. Nakao,[14, 10] T. Nanut,[24] N. K. Nisar,[57] S. Nishida,[14, 10] S. Okuno,[25] W. Ostrowicz,[46] C. W. Park,[54] H. Park,[31] T. K. Pedlar,[34] R. Pestotnik,[24] M. Petrič,[24] L. E. Piilonen,[64] E. Ribežl,[24] M. Ritter,[36] A. Rostomyan,[8] Y. Sakai,[14, 10] S. Sandilya,[57] L. Santelj,[24] T. Sanuki,[59] O. Schneider,[32] G. Schnell,[1, 15] C. Schwanda,[20] D. Semmler,[9] K. Senyo,[66] V. Shebalin,[4] T.-A. Shibata,[61] J.-G. Shiu,[45] B. Shwartz,[4] A. Sibidanov,[55] F. Simon,[36, 58] Y.-S. Sohn,[67] A. Sokolov,[21] M. Starič,[24] M. Steder,[8] T. Sumiyoshi,[62] U. Tamponi,[22, 63] K. Tanida,[52] G. Tatishvili,[49] Y. Teramoto,[48] M. Uchida,[61] S. Uehara,[14, 10] T. Uglov,[23, 39] Y. Unno,[12] S. Uno,[14, 10] P. Urquijo,[3] Y. Usov,[4] S. E. Vahsen,[13] C. Van Hulse,[1] P. Vanhoefer,[36] G. Varner,[13] A. Vinokurova,[4] V. Vorobyev,[4] A. Vossen,[18] M. N. Wagner,[9] C. H. Wang,[44] M.-Z. Wang,[45] P. Wang,[19] X. L. Wang,[64] M. Watanabe,[47] Y. Watanabe,[25] E. Won,[30] J. Yamaoka,[49] S. Yashchenko,[8] Y. Yook,[67] C. Z. Yuan,[19] Z. P. Zhang,[51] V. Zhilich,[4] and V. Zhulanov[4]

(The Belle Collaboration)

[1] *University of the Basque Country UPV/EHU, 48080 Bilbao*

[2] *Beihang University, Beijing 100191*

[3] *University of Bonn, 53115 Bonn*

[4] *Budker Institute of Nuclear Physics SB RAS and Novosibirsk State University, Novosibirsk 630090*

[5]*Faculty of Mathematics and Physics, Charles University, 121 16 Prague*

[6]*Chonnam National University, Kwangju 660-701*

[7]*University of Cincinnati, Cincinnati, Ohio 45221*

[8]*Deutsches Elektronen–Synchrotron, 22607 Hamburg*

[9]*Justus-Liebig-Universität Gießen, 35392 Gießen*

[10]*The Graduate University for Advanced Studies, Hayama 240-0193*

[11]*Gyeongsang National University, Chinju 660-701*

[12]*Hanyang University, Seoul 133-791*

[13]*University of Hawaii, Honolulu, Hawaii 96822*

[14]*High Energy Accelerator Research Organization (KEK), Tsukuba 305-0801*

[15]*IKERBASQUE, Basque Foundation for Science, 48011 Bilbao*

[16]*Indian Institute of Technology Guwahati, Assam 781039*

[17]*Indian Institute of Technology Madras, Chennai 600036*

[18]*Indiana University, Bloomington, Indiana 47408*

[19]*Institute of High Energy Physics, Chinese Academy of Sciences, Beijing 100049*

[20]*Institute of High Energy Physics, Vienna 1050*

[21]*Institute for High Energy Physics, Protvino 142281*

[22]*INFN - Sezione di Torino, 10125 Torino*

[23]*Institute for Theoretical and Experimental Physics, Moscow 117218*

[24]*J. Stefan Institute, 1000 Ljubljana*

[25]*Kanagawa University, Yokohama 221-8686*

[26]*Institut für Experimentelle Kernphysik, Karlsruher Institut für Technologie, 76131 Karlsruhe*

[27]*Kennesaw State University, Kennesaw GA 30144*

[28]*Department of Physics, Faculty of Science, King Abdulaziz University, Jeddah 21589*

[29]*Korea Institute of Science and Technology Information, Daejeon 305-806*

[30]*Korea University, Seoul 136-713*

[31]*Kyungpook National University, Daegu 702-701*

[32]*École Polytechnique Fédérale de Lausanne (EPFL), Lausanne 1015*

[33]*Faculty of Mathematics and Physics, University of Ljubljana, 1000 Ljubljana*

[34]*Luther College, Decorah, Iowa 52101*

[35]*University of Maribor, 2000 Maribor*

[36]*Max-Planck-Institut für Physik, 80805 München*

[37]*School of Physics, University of Melbourne, Victoria 3010*

[38]*Moscow Physical Engineering Institute, Moscow 115409*

[39]*Moscow Institute of Physics and Technology, Moscow Region 141700*

[40]*Graduate School of Science, Nagoya University, Nagoya 464-8602*

[41]*Kobayashi-Maskawa Institute, Nagoya University, Nagoya 464-8602*

[42] *Nara Women's University, Nara 630-8506*

[43] *National Central University, Chung-li 32054*

[44] *National United University, Miao Li 36003*

[45] *Department of Physics, National Taiwan University, Taipei 10617*

[46] *H. Niewodniczanski Institute of Nuclear Physics, Krakow 31-342*

[47] *Niigata University, Niigata 950-2181*

[48] *Osaka City University, Osaka 558-8585*

[49] *Pacific Northwest National Laboratory, Richland, Washington 99352*

[50] *Peking University, Beijing 100871*

[51] *University of Science and Technology of China, Hefei 230026*

[52] *Seoul National University, Seoul 151-742*

[53] *Soongsil University, Seoul 156-743*

[54] *Sungkyunkwan University, Suwon 440-746*

[55] *School of Physics, University of Sydney, NSW 2006*

[56] *Department of Physics, Faculty of Science, University of Tabuk, Tabuk 71451*

[57] *Tata Institute of Fundamental Research, Mumbai 400005*

[58] *Excellence Cluster Universe, Technische Universität München, 85748 Garching*

[59] *Tohoku University, Sendai 980-8578*

[60] *Department of Physics, University of Tokyo, Tokyo 113-0033*

[61] *Tokyo Institute of Technology, Tokyo 152-8550*

[62] *Tokyo Metropolitan University, Tokyo 192-0397*

[63] *University of Torino, 10124 Torino*

[64] *CNP, Virginia Polytechnic Institute and State University, Blacksburg, Virginia 24061*

[65] *Wayne State University, Detroit, Michigan 48202*

[66] *Yamagata University, Yamagata 990-8560*

[67] *Yonsei University, Seoul 120-749*

Using data samples of 102×10^6 $\Upsilon(1S)$ and 158×10^6 $\Upsilon(2S)$ events collected with the Belle detector, a first experimental search has been made for double-charmonium production in the exclusive decays $\Upsilon(1S, 2S) \to J/\psi(\psi') + X$, where $X = \eta_c$, $\chi_{cJ}(J = 0, 1, 2)$, $\eta_c(2S)$, $X(3940)$, and $X(4160)$. No significant signal is observed in the spectra of the mass recoiling against the reconstructed J/ψ or ψ' except for the evidence of χ_{c1} production with a significance of 4.6σ for $\Upsilon(1S) \to J/\psi + \chi_{c1}$. The measured branching fraction $\mathcal{B}(\Upsilon(1S) \to J/\psi + \chi_{c1})$ is $(3.90 \pm 1.21(\text{stat.}) \pm 0.23(\text{syst.})) \times 10^{-6}$. The 90% confidence level upper limits on the branching fractions of the other modes having a significance of less than 3σ are determined. These results are consistent with theoretical calculations using the nonrelativistic QCD factorization approach.

PACS numbers: 13.25.Gv, 13.25.Hw, 14.40.Pq

For many years, one of the largest discrepancies in quarkonium physics has been the unexpected disagreement between the experimental measurements and theoretical predictions for double-charmonium production at B factories. The cross sections of the processes $e^+e^- \to J/\psi\eta_c$, $J/\psi\eta_c(2S)$, $\psi'\eta_c$, $\psi'\eta_c(2S)$, $J/\psi\chi_{c0}$, and $\psi'\chi_{c0}$ measured by the Belle [1, 2] and BaBar [3] Collaborations exceeded the leading-order non-relativistic QCD (NRQCD) calculations by approximately an order of magnitude [4–9]. Later the double-charmonium productions of $J/\psi X(3940)$ [10, 11] and $J/\psi X(4160)$ [12] were observed in e^+e^- annihilation by Belle as well. Numerous theoretical investigations in the following years had attempted to alleviate this disquieting discrepancy, and it is now believed that one can achieve agreement within reasonable uncertainties when both the QCD radiative and relativistic corrections of the order of v^2 (where v is the quark relative velocity) are taken into account [13–21].

Inspired by the unexpectedly high double-charmonium production in e^+e^- annihilation, interest has turned to the double-charmonium states produced in bottomonium decays. Several theoretical calculations have focused on these processes in perturbative QCD, e.g., $\eta_b \to J/\psi J/\psi$ [22–25] and $\chi_{b0,1,2} \to J/\psi J/\psi$ [26–29]. Experimentally, however, such studies are extremely sparse, apart from the recent searches for several channels of χ_{bJ} into double charmonia for the first time by the Belle Collaboration [30]. The measurements are consistent with NRQCD predictions, though no significant signals are observed; it is reasonable to extend the search for double-charmonium production to the C-odd Υ decays. Compared with the $\Upsilon(4S)$ resonance with its rather broad width, the first three Υ resonances are so narrow that the resonant decay contributions dominate over the continuum ones. This provides a further opportunity to probe the potential properties of double-charmonium production at these Υ peaks.

Comprehensive studies of the exclusive decay of Υ into a vector-plus-pseudoscalar charmonium [31], as well as the S-wave charmonium J/ψ plus the P-wave charmonium χ_{cJ} ($J = 0$, 1, 2) [32] have been performed in the NRQCD factorization approach, where the contributions from the strong, electromagnetic, and radiative channels were considered and the strong decay was taken as dominant. The branching fractions are predicted to be of order 10^{-6} for $\Upsilon(nS) \to J/\psi(\psi') + \eta_c(\eta_c(2S))$ ($n = 1$, 2, 3) [31]; for $\Upsilon \to J/\psi + \eta_c$, in particular, the predicted branching fraction is consistent with the previous calculation of 1.7×10^{-6} with only the three-gluon contribution considered [33]. For the $J/\psi + \chi_{c0,1,2}$ decay modes, the branching fractions are calculated at the lowest order [32]; that of $\Upsilon(nS) \to J/\psi + \chi_{c1}$ is the largest—of order 10^{-6}—while that of $J/\psi + \chi_{c2}$ is only of order 10^{-7}. In this paper, we report studies of exclusive hadronic decays of $\Upsilon(1S)$ and $\Upsilon(2S)$ resonances to the double-charmonium final states $J/\psi(\psi') + X$, where X

is one of the η_c, χ_{cJ} ($J = 0,\ 1,\ 2$), $\eta_c(2S)$, $X(3940)$, and $X(4160)$ states. To improve the signal detection efficiencies, only the J/ψ or ψ' candidate is fully reconstructed; we search for the other charmonium state X in the recoil mass distribution of the fully reconstructed J/ψ or ψ' candidate. The recoil mass is calculated as $M_{\text{recoil}}(c\bar{c}) = \sqrt{(E_{\text{CM}} - E_{c\bar{c}}^*)^2 - p_{c\bar{c}}^{*2}c^2}/c^2$, where $c\bar{c}$ is the reconstructed charmonium J/ψ or ψ', $E_{c\bar{c}}^*$ and $p_{c\bar{c}}^*$ are the center-of-mass (CM) energy and momentum of $J/\psi(\psi')$ and E_{CM} is the center-of-mass energy of the colliding e^+e^- system.

This analysis utilizes the $\Upsilon(1S)$ and $\Upsilon(2S)$ samples from Belle with a total luminosity of $5.74\,\text{fb}^{-1}$ (102×10^6 events) and $24.91\,\text{fb}^{-1}$ (158×10^6 events), respectively. A $89.45\,\text{fb}^{-1}$ data sample collected at $\sqrt{s} = 10.52$ GeV is used to estimate the possible irreducible continuum contributions. All data were collected with the Belle detector [34, 35] operating at the KEKB asymmetric-energy e^+e^- collider [36, 37]. The signal Monte Carlo (MC) events are generated with EVTGEN [38] using the helicity-amplitude model [31, 32]. The decays of the two charmonium daughters are generated according to the known branching fractions [39], while unknown decay channels are generated by the Lund fragmentation model in PYTHIA [40]. Generic decay samples of $\Upsilon(1S)$ and $\Upsilon(2S)$ MC events produced using PYTHIA [40] with four times the luminosity of the data, are used to identify possible peaking backgrounds from $\Upsilon(1S)$ and $\Upsilon(2S)$ decays.

The Belle detector is a large solid angle magnetic spectrometer that consists of a silicon vertex detector (SVD), a 50-layer central drift chamber (CDC), an array of aerogel threshold Cherenkov counters (ACC), a barrel-like arrangement of time-of-flight scintillation counters (TOF), and an electromagnetic calorimeter comprising CsI(Tl) crystals located inside a superconducting solenoid coil that provides a 1.5 T magnetic field. An iron flux return located outside the coil is instrumented to detect K_L^0 mesons and to identify muons. A detailed description of the Belle detector can be found in Ref. [34].

Primary charged tracks are selected with $dr < 2$ cm and $|dz| < 4$ cm, where dr and dz are the impact parameters perpendicular to and along the beam direction with respect to the interaction point. In addition, the transverse momentum of every charged track in the laboratory frame is restricted to be larger than 0.1 GeV/c. QED backgrounds are significantly suppressed by the requirement that the charged multiplicity (N_{ch}) in every event satisfies $N_{\text{ch}} > 4$ [2]. Lepton candidate tracks from $J/\psi(\psi')$ are required to have a muon likelihood ratio $R_\mu = \frac{\mathcal{L}_\mu}{\mathcal{L}_\mu + \mathcal{L}_K + \mathcal{L}_\pi} > 0.1$ [41] or an electron likelihood ratio $R_e = \frac{\mathcal{L}_e}{\mathcal{L}_e + \mathcal{L}_{non-e}} > 0.01$ [42]. To reduce the effect of bremsstrahlung and final-state radiation, photons detected in the ECL within a 50 mrad cone of the original electron or positron direction are included in the calculation of the e^+/e^- four-momentum. The lepton-identification efficiencies for $e^\pm$ and $\mu^\pm$ are about 98% and 96%, respectively. Because

ψ' is also reconstructed from $J/\psi\pi^+\pi^-$, charged tracks with $R_K = \frac{\mathcal{L}_K}{\mathcal{L}_K + \mathcal{L}_\pi} < 0.4$ [43] are considered to be pions for this purpose, with an efficiency of about 98% and a kaon misidentification rate of about 2.6%.

When reconstructing $J/\psi(\psi')$ candidates for all the modes, a mass-constrained fit is applied to improve the resolutions of the recoil mass distributions. MC simulations indicate that the $J/\psi(\psi')$ has almost the same mass resolution if the $J/\psi(\psi')$ is reconstructed from the same final states in $\Upsilon(1S, 2S) \to J/\psi(\psi') + X$ processes. The signal region for J/ψ is defined as $|M_{\ell^+\ell^-} - m_{J/\psi}| <$ 0.03 GeV/c^2 ($\sim 2.5\sigma$), where $\ell = e$ or μ and $m_{J/\psi}$ is the nominal mass of the J/ψ [39]; the J/ψ mass sidebands are defined as 2.97 GeV/c^2 < $M_{\ell^+\ell^-}$ < 3.03 GeV/c^2 or 3.17 GeV/c^2 < $M_{\ell^+\ell^-}$ < 3.23 GeV/c^2. For ψ' candidates with $\ell^+\ell^-$ and $J/\psi\pi^+\pi^-$ final states, the ψ' signal regions are defined as $|M_{\ell^+\ell^-} - m_{\psi'}| < 0.0375$ GeV/c^2 ($\sim 2.5\sigma$) and $|M_{J/\psi\pi^+\pi^-} - m_{\psi'}| < 0.009$ GeV/c^2 ($\sim$ 3.0σ), respectively, where $m_{\psi'}$ is the nominal mass of the ψ' [39]. The ψ' mass sidebands are defined as 3.535 GeV/c^2 < $M_{\ell^+\ell^-}$ < 3.610 GeV/c^2 or 3.760 GeV/c^2 < $M_{\ell^+\ell^-}$ < 3.835 GeV/c^2, and 3.652 GeV/c^2 < $M_{J/\psi\pi^+\pi^-}$ < 3.670 GeV/c^2 or 3.700 GeV/c^2 < $M_{J/\psi\pi^+\pi^-}$ < 3.718 GeV/c^2. The mass sidebands of both the J/ψ and ψ' are twice as wide as the signal region. Figure 1 shows the mass distributions of the reconstructed $J/\psi(\to \ell^+\ell^-)$, $\psi'(\to \ell^+\ell^-)$, and $\psi'(\to J/\psi\pi^+\pi^-)$ candidates in $\Upsilon(1S)$ and $\Upsilon(2S)$ decays. The signal regions of the J/ψ and ψ' candidates are indicated with arrows in the corresponding graphs. The analysis region of the recoil masses is 2.2 GeV/c^2 < $M_{\mathrm{recoil}}(J/\psi(\psi'))$ < 4.6 GeV/c^2 and covers all the recoil charmonium states of interest.

After all event selections, no peaking background in any charmonium signal region is found from the $\Upsilon(1S)$ or $\Upsilon(2S)$ generic MC samples. Typical Υ decay samples include three categories: Υ decay signal events, Υ decay background events, and continuum events. The backgrounds with non-$J/\psi(\psi')$ from Υ decay are estimated by normalizing the $J/\psi(\psi')$ mass sideband events to their signal regions. The large continuum data sample at $\sqrt{s} = 10.52$ GeV is used to estimate the continuum contributions in our data samples by extrapolating down to the $\Upsilon(1S)$ or $\Upsilon(2S)$ resonance. The scale factor of the extrapolation is computed with $f_{\mathrm{scale}} = \frac{\mathcal{L}_\Upsilon}{\mathcal{L}_{\mathrm{con}}} \frac{\sigma_\Upsilon}{\sigma_{\mathrm{con}}} \frac{\varepsilon_\Upsilon}{\varepsilon_{\mathrm{con}}}$, where $\frac{\mathcal{L}_\Upsilon}{\mathcal{L}_{\mathrm{con}}}$, $\frac{\sigma_\Upsilon}{\sigma_{\mathrm{con}}}$, and $\frac{\varepsilon_\Upsilon}{\varepsilon_{\mathrm{con}}}$ are the ratios of the luminosity, cross sections, and efficiencies, respectively, at the Υ and continuum points. For the nominal results, the efficiencies are obtained from MC simulations; their ratios in Υ and continuum events are equal for all decay modes of $J/\psi(\psi')$ and the cross sections of the target channels are scaled to be proportional to $1/s^4$ ($\sqrt{s} = E_{\mathrm{CM}}$) [4, 44]; the corresponding scale factors are about 0.16 and 0.44 for $\Upsilon(1S)$ and $\Upsilon(2S)$, respectively.

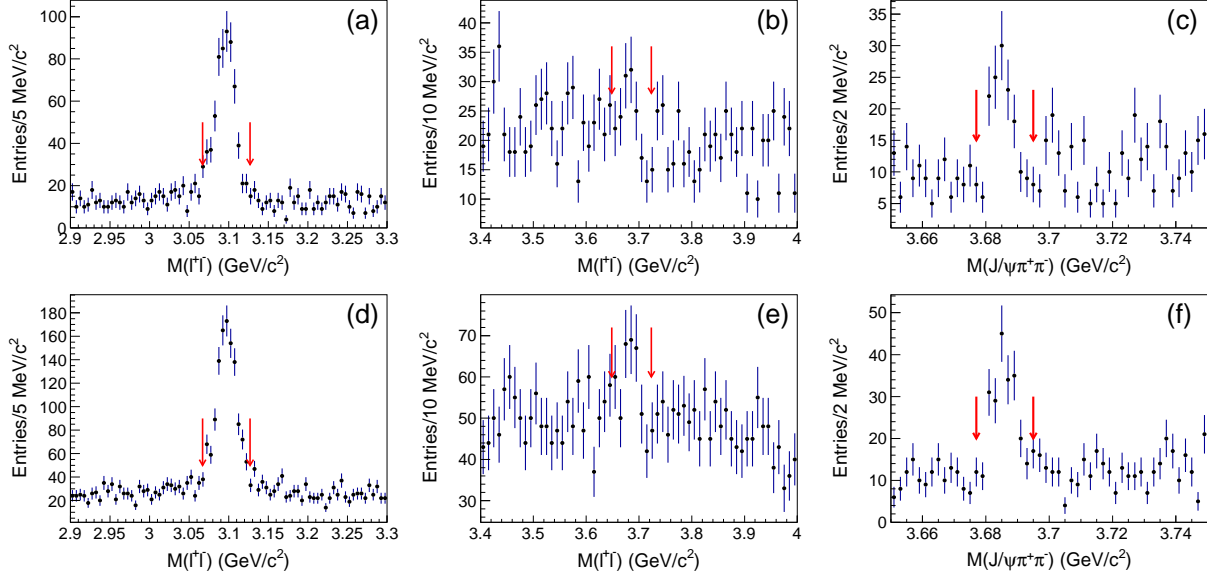Figure 2 shows the distributions of the recoil masses against the reconstructed $J/\psi(\to \ell^+\ell^-)$,

FIG. 1. Distributions of the invariant masses of J/ψ identified with lepton pairs, and ψ' identified with both $\ell^+\ell^-$ and $J/\psi\pi^+\pi^-$ with the $J/\psi(\psi')$ recoil mass within 2.2 GeV/c^2 and 4.6 GeV/c^2 from left to right. The upper and lower three graphs are for $\Upsilon(1S)$ and $\Upsilon(2S)$ decays, respectively. The arrows show the signal regions of J/ψ or ψ' masses.
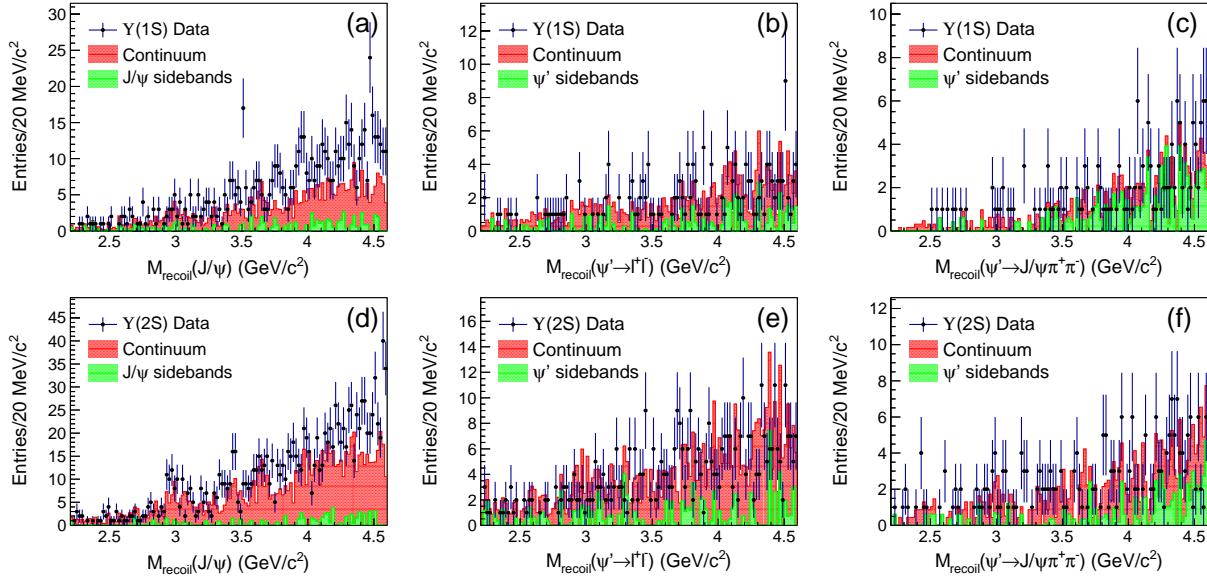

FIG. 2. Distributions of the recoil masses against the reconstructed $J/\psi(\to \ell^+\ell^-)$, $\psi'(\to \ell^+\ell^-)$, $\psi'(\to J/\psi\pi^+\pi^-)$ within the J/ψ or ψ' mass signal regions from left to right. The upper and lower three graphs are for $\Upsilon(1S)$ and $\Upsilon(2S)$ decays, respectively. The red-shaded histograms are from the normalized continuum sample at $\sqrt{s} = 10.52$ GeV, and the green ones represent the scaled $J/\psi(\psi')$ mass sideband backgrounds from Υ decays.

$\psi'(\to \ell^+\ell^-)$, and $\psi'(\to J/\psi\pi^+\pi^-)$ within their signal regions. The upper (lower) three graphs are

for the $\Upsilon(1S)$ ($\Upsilon(2S)$) decays. The green-shaded histograms are the scaled $J/\psi(\psi')$ mass sideband backgrounds from Υ decays. Contributions from e^+e^- annihilation with the same final states have been subtracted from the sideband distributions to avoid double-counting of continuum events. The red-shaded histograms represent the normalized continuum backgrounds, whose estimation is described in the previous paragraph. In the spectrum of the J/ψ recoil mass in $\Upsilon(1S)$ decays in Fig. 2(a), the sharp peak that appears at 3.51 GeV/c^2 is likely to be that of the χ_{c1}, for which the width is as narrow as 0.86 MeV/c^2 [39]. A slight enhancement around 3.94 GeV/c^2 may also be seen; no other distinct charmonium signal is observed. For the $\psi' \to \ell^+\ell^-$ mode in Fig. 2(b) and $\psi' \to J/\psi\pi^+\pi^-$ mode in Fig. 2(c), the ψ' mass sidebands and continuum backgrounds together contribute essentially all the events within the ψ' signal region. The J/ψ recoil mass distribution in Fig. 2(d) reveals weak possible signals around the nominal masses of the η_c, χ_{c0} and $\eta_c(2S)$ in $\Upsilon(2S)$ decays. However, after subtracting the continuum contribution, the surviving events are consistent with the combinatorial background. Similarly to the two ψ' decay modes in $\Upsilon(1S)$ decays, only backgrounds are found in the ψ' recoil mass distributions for the $\Upsilon(2S)$ decays, as shown in Figs. 2(e) and 2(f).

Another background in $\Upsilon(2S)$ decays is the intermediate transition $\Upsilon(2S) \to \pi^+\pi^-\Upsilon(1S)$ or $\pi^0\pi^0\Upsilon(1S)$ with $\Upsilon(1S)$ decaying into double charmonia. Such contamination is examined with the recoil masses of additionally selected $\pi^+\pi^-$ or $\pi^0\pi^0$ pairs to check for $\Upsilon(1S)$ signals. After all event selections, the ratios of such backgrounds are $(9.6 \pm 1.7)\%$ and $(15.0 \pm 2.8)\%$ for the $J/\psi + X$ and $\psi' + X$ processes, respectively, by fitting the recoil mass spectra of $\pi^0\pi^0$ and $\pi^+\pi^-$ pairs. However, the corresponding distribution of the mass recoiling against the $J/\psi(\psi')$ is smooth; therefore, the contamination is non-peaking. Here, a π^0 candidate is reconstructed from a pair of good photons [45] with an invariant mass within 15 MeV/c^2 of the π^0 nominal mass. We require $\chi^2 < 20$, where χ^2 is from the mass-constrained fit of $\pi^0 \to \gamma\gamma$.

An unbinned extended simultaneous likelihood fit is applied to the spectra of the mass recoiling against the J/ψ or ψ' to extract the signal yields in the $\Upsilon(1S, 2S)$ and continuum data samples. For $\psi' + X$ processes, the decay modes $\psi' \to \ell^+\ell^-$ and $\psi' \to J/\psi\pi^+\pi^-$ are treated together to obtain the total yield of every ψ' recoil $c\bar{c}$ signal. That is to say, in the fit to the ψ' recoil mass spectra, in addition to the simultaneous fit applied to the Υ and continuum data samples, we also apply a simultaneous fit to these two ψ' decay modes. The ratio of any charmonium-like yields between the $\psi' \to \ell^+\ell^-$ and $\psi' \to J/\psi\pi^+\pi^-$ modes is fixed to the ratio of the MC-determined efficiencies between these two ψ' decay modes with all the intermediate-state branching fractions included.

The signal shapes of all the recoil $c\bar{c}$ states are determined from MC simulations with the mass resolutions of 31 MeV/c^2, 24 MeV/c^2, 23 MeV/c^2, 19 MeV/c^2, and 18 MeV/c^2 for the recoiling η_c, χ_{cJ}, $\eta_c(2S)$, $X(3940)$, and $X(4160)$, respectively. In the MC simulations, for all the recoil $c\bar{c}$ states, the world-average resonance parameters are used with masses fixed at 2.984 GeV/c^2, 3.097 GeV/c^2, 3.415 GeV/c^2, 3.511 GeV/c^2, 3.556 GeV/c^2, 3.639 GeV/c^2, 3.942 GeV/c^2 and 4.156 GeV/c^2 for η_c, J/ψ, χ_{c0}, χ_{c1}, χ_{c2}, $\eta_c(2S)$, $X(3940)$, and $X(4160)$, respectively [39]. Because of the production-channel dependence of the transition matrix element for a description of the η_c line shape [46], a smearing Gaussian function with free parameters is introduced there to improve the fit accuracy and to account for possible discrepancies between data and MC . In other words, the η_c shape is described with the MC-determined shape convolved with this Gaussian function. The other $c\bar{c}$ signals are described directly by the MC-determined shapes. In the fit to the Υ candidates, a Chebychev polynomial background shape is used for the $\Upsilon(1S, 2S)$ decay backgrounds in addition to the normalized continuum contribution. Since the fit range includes the region over the $D\bar{D}$ threshold ($\approx$ 3.73 GeV/c^2), a threshold term proportional to $(M_{\mathrm{recoil}}(c\bar{c}) - 2m_D)^n$ is added, where n is a free parameter and m_D is the D meson nominal mass. This term is added in the background parametrization with a free normalization to account for the possible contribution from $\Upsilon(1S, 2S)/e^+e^- \to J/\psi(\psi')D^{(*)}\bar{D}^{(*)}$.

The fit range and results to the spectra of the recoil mass against J/ψ and ψ' are shown in Figs. 3 and 4 from the $\Upsilon(1S)$ and $\Upsilon(2S)$ data samples, respectively. The points with error bars represent the $\Upsilon(1S, 2S)$ events. The red solid curves give the nominal fit results while the blue-dashed curves are the estimated total background. The cyan-shaded histograms are the fitted normalized continuum contributions under the $J/\psi(\psi')$ signal region. The fitted signal yields (N_{fit}) of every recoil charmonium state are listed in Table I.

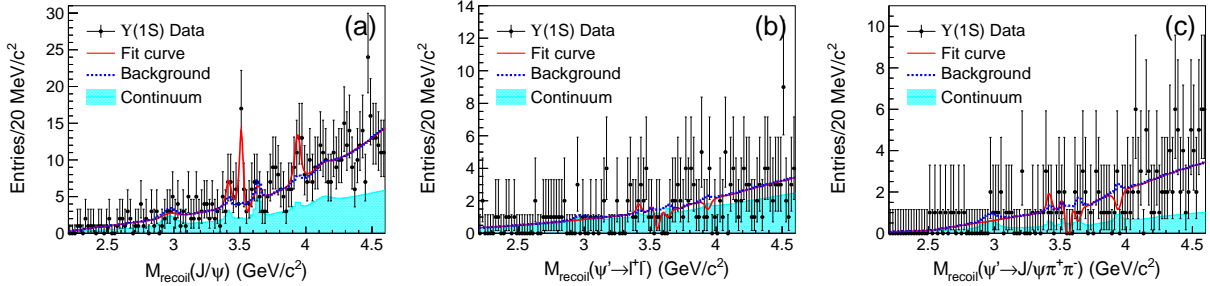
FIG. 3. Fit to the recoil mass spectra against the (a) $J/\psi(\to \ell^+\ell^-)$, (b) $\psi'(\to \ell^+\ell^-)$ and (c) $\psi'(\to J/\psi\pi^+\pi^-)$ in $\Upsilon(1S)$ decays from data (points with error bars). The red solid curves are the nominal fits and the blue-dashed curves show the total background. The fitted normalized continuum contributions are represented by the cyan-shaded histograms.

TABLE I. Results of the search for $\Upsilon(1S)$ and $\Upsilon(2S)$ decays into double charmonia. For each decay mode, N_{fit} represents the number of fitted signal events, N_{up} is the upper limit on the number of signal events, ε is the reconstruction efficiency, σ_{syst} is the total systematic error, Σ is the signal significance with systematic error included, $\mathcal{B}_R$ is the measured branching fraction where the upper limit is at 90% C.L., and $\mathcal{B}_{\text{th}}$ is taken from the theoretical predictions [31, 32].

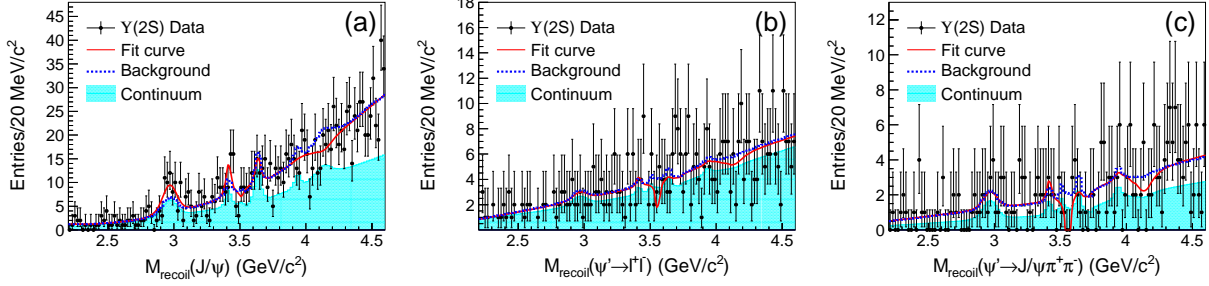| Channels	N_{fit}	N_{up}	$\varepsilon(\%)$	$\sigma_{syst}(\%)$	$\Sigma\ (\sigma)$	$\mathcal{B}_R(\times 10^{-6})$	$\mathcal{B}_{\text{th}}(\times 10^{-6})$
$\Upsilon(1S) \to J/\psi + \eta_c$	-4.9 ± 6.3	8.1	3.71	8.1	$-$	< 2.2	$3.9^{+5.6}_{-2.3}$
$\Upsilon(1S) \to J/\psi + \chi_{c0}$	6.0 ± 5.6	14.4	4.25	5.1	1.3	< 3.4	1.3
$\Upsilon(1S) \to J/\psi + \chi_{c1}$	19.9 ± 6.2	$-$	4.98	5.9	4.6	$3.90 \pm 1.21 \pm 0.23$	4.9
$\Upsilon(1S) \to J/\psi + \chi_{c2}$	-3.2 ± 4.0	6.4	4.71	4.7	$-$	< 1.4	0.20
$\Upsilon(1S) \to J/\psi + \eta_c(2S)$	-2.2 ± 6.0	9.3	4.32	5.2	$-$	< 2.2	$2.0^{+3.4}_{-1.4}$
$\Upsilon(1S) \to J/\psi + X(3940)$	18.4 ± 8.8	30.9	5.67	8.4	2.6	< 5.4	$-$
$\Upsilon(1S) \to J/\psi + X(4160)$	-0.7 ± 15.0	22.7	5.28	19.7	$-$	< 5.4	$-$
$\Upsilon(1S) \to \psi' + \eta_c$	-4.6 ± 4.0	5.8	1.58	13.5	$-$	< 3.6	$1.7^{+2.4}_{-1.0}$
$\Upsilon(1S) \to \psi' + \chi_{c0}$	2.5 ± 4.2	10.6	1.60	17.7	0.7	< 6.5	$-$
$\Upsilon(1S) \to \psi' + \chi_{c1}$	0.6 ± 3.7	7.9	1.68	21.5	0.2	< 4.5	$-$
$\Upsilon(1S) \to \psi' + \chi_{c2}$	-6.5 ± 2.4	3.5	1.64	7.1	$-$	< 2.1	$-$
$\Upsilon(1S) \to \psi' + \eta_c(2S)$	-5.4 ± 3.6	5.3	1.68	20.5	$-$	< 3.2	$0.8^{+1.4}_{-0.6}$
$\Upsilon(1S) \to \psi' + X(3940)$	-6.7 ± 4.0	5.6	1.92	11.8	$-$	< 2.9	$-$
$\Upsilon(1S) \to \psi' + X(4160)$	-0.3 ± 10.3	17.2	1.86	21.8	$-$	< 2.9	$-$
$\Upsilon(2S) \to J/\psi + \eta_c$	18.8 ± 11.8	35.7	3.61	16.9	2.2	< 5.4	$2.6^{+3.7}_{-1.6}$
$\Upsilon(2S) \to J/\psi + \chi_{c0}$	9.3 ± 9.4	21.5	4.17	6.4	1.3	< 3.4	1.1
$\Upsilon(2S) \to J/\psi + \chi_{c1}$	-4.0 ± 6.5	8.4	4.95	5.8	$-$	< 1.2	4.1
$\Upsilon(2S) \to J/\psi + \chi_{c2}$	2.3 ± 7.4	13.1	4.57	6.8	0	< 2.0	0.17
$\Upsilon(2S) \to J/\psi + \eta_c(2S)$	-4.7 ± 10.8	13.7	4.23	10.4	$-$	< 2.5	$1.3^{+2.1}_{-0.9}$
$\Upsilon(2S) \to J/\psi + X(3940)$	-8.8 ± 11.9	14.0	5.65	16.3	$-$	< 2.0	$-$
$\Upsilon(2S) \to J/\psi + X(4160)$	-40.3 ± 22.2	14.9	5.37	18.6	$-$	< 2.0	$-$
$\Upsilon(2S) \to \psi' + \eta_c$	-1.4 ± 8.4	11.9	1.56	8.6	$-$	< 5.1	$1.1^{+1.6}_{-0.7}$
$\Upsilon(2S) \to \psi' + \chi_{c0}$	1.6 ± 6.1	11.3	1.63	8.2	0.3	< 4.7	$-$
$\Upsilon(2S) \to \psi' + \chi_{c1}$	-3.7 ± 4.5	6.2	1.66	6.9	$-$	< 2.5	$-$
$\Upsilon(2S) \to \psi' + \chi_{c2}$	-13.5 ± 5.2	4.9	1.66	6.9	$-$	< 1.9	$-$
$\Upsilon(2S) \to \psi' + \eta_c(2S)$	-5.0 ± 6.6	8.0	1.66	7.7	$-$	< 3.3	$0.5^{+0.9}_{-0.4}$
$\Upsilon(2S) \to \psi' + X(3940)$	-2.0 ± 7.3	10.7	1.96	7.9	$-$	< 3.9	$-$
$\Upsilon(2S) \to \psi' + X(4160)$	-13.1 ± 14.0	12.4	1.89	10.9	$-$	< 3.9	$-$

FIG. 4. Fit to the recoil mass spectra against (a) $J/\psi(\to \ell^+\ell^-)$, (b) $\psi'(\to \ell^+\ell^-)$ and (c) $\psi'(\to J/\psi\pi^+\pi^-)$ in $\Upsilon(2S)$ decays from data (points with error bars). The representations of the curves and histograms in each graph match those in Fig. 3.

Several sources of systematic errors are taken into account in the branching fraction measurements. Tracking efficiency uncertainty is estimated to be 0.35% per track with high momentum and is additive. Based on the measurements of the identification efficiencies of the lepton pair with $\gamma\gamma \to \ell^+\ell^-$ and the pion using the D^* sample, the MC simulates data with uncertainties within about 1.8% and 1.3% for each lepton and pion, respectively. As the trigger efficiency evaluated from a trigger simulation is greater than 99.9%, its uncertainty can be neglected. The errors on the branching fractions of the intermediate states are taken from the Particle Data Group [39], which are about 1.1%, 6.3% and 1.2% for $J/\psi \to \ell^+\ell^-$, $\psi' \to \ell^+\ell^-$ and $\psi' \to J/\psi\pi^+\pi^-$, respectively; the weighted average for the two ψ' decay modes is about 3.5%. For the charmonium states with generic decays, the unknown decay channels are generated by the Lund fragmentation model in PYTHIA [40]. By generating different sets of MC samples with different relative probabilities to produce the various possible $q\bar{q}$ ($q = u$, d, s) pairs, the largest difference in the efficiencies is found to be less than 0.1% and thus is neglected. The uncertainty due to the $N_{ch} > 4$ requirement is at the 1.0% level, determined by changing the known decay branching fractions of recoil charmonium states to the final states with $N_{ch} < 5$ by 1σ [39]. By varying the background shapes or the order of the Chebychev polynomial, as well as the fitted range and the width of the smearing Gaussian within $\pm1\sigma$, the deviation of the upper limits on the number of the signal events is found to be between 2.0% and 24.1%, depending on the decay mode. The MC statistical errors are estimated using the reconstruction efficiencies and the number of generated events, which are at most 1.8%. The uncertainties associated with the total number of $\Upsilon(1S)$ and $\Upsilon(2S)$ events are 2.0% and 2.3%, respectively. Assuming that all the sources are independent and summed in quadrature, the total systematic errors (σ_{syst}) are evaluated and listed in Table I.

Since few distinct signals are observed, the upper limit on the number of signal events (N_{up}) is

determined at the 90% confidence level (C.L.) by solving the equation $\int_0^{N_{\mathrm{up}}} \mathcal{L}(x)dx / \int_0^{+\infty} \mathcal{L}(x)dx =$ 0.9, where x is the number of fitted signal events and $\mathcal{L}(x)$ is the likelihood function in the fit to the data, convolved here with a Gaussian function whose width equals the total systematic uncertainty. The value of N_{up} for each mode, which requires the signal yields to be non-negative in the fit, is listed in Table I along with the corresponding calculated branching fraction ($\mathcal{B}_R$) or its upper limit. The theoretical predictions ($\mathcal{B}_{\mathrm{th}}$) from Refs. [31, 32] are also tabulated. Due to the sensitivity to the choices of some parameters such as the charm-quark mass (m_c), NRQCD matrix elements, and QCD coupling constant (α_s), the central values of $\mathcal{B}_{\mathrm{th}}$ have large uncertainties. Table I also lists the reconstruction efficiency (ε) and the signal significance (Σ) that is obtained by calculating $\sqrt{-2\ln(\mathcal{L}_0/\mathcal{L}_{\mathrm{max}})}$, where $\mathcal{L}_0$ and $\mathcal{L}_{\mathrm{max}}$ are the likelihoods of the fits without and with a signal component, respectively. Here, for the likelihood function the width of the convolved Gaussian equals the systematic uncertainty related to signal yield instead of the total systematic uncertainty.

To summarize, we have performed a first experimental investigation into double-charmonium production in $\Upsilon(1S, 2S)$ decays by using the Belle data samples of 102×10^6 $\Upsilon(1S)$ and 158×10^6 $\Upsilon(2S)$ events. The evidence for the mode $\Upsilon(1S) \to J/\psi + \chi_{c1}$ is found, for which the branching fraction is measured to be $\mathcal{B}(\Upsilon(1S) \to J/\psi + \chi_{c1}) = (3.90 \pm 1.21(\text{stat.}) \pm 0.23(\text{syst.})) \times 10^{-6}$ ($< 5.7 \times 10^{-6}$ at 90% C.L.) with a signal significance of 4.6σ. The 90% C.L. upper limits are set on the branching fractions of the other decays of $\Upsilon(1S, 2S)$ into double-charmonium states that have a signal significance of less than 3σ. Our results are found to be consistent with the theoretical calculations made using the NRQCD factorization approach [31, 32].

[1] K. Abe *et al.* (Belle Collaboration), Phys. Rev. Lett. **89**, 142001 (2002).

[2] K. Abe *et al.* (Belle Collaboration), Phys. Rev. D **70**, 071102(R) (2004).

[3] B. Aubert *et al.* (BaBar Collaboration), Phys. Rev. D **72**, 031101(R) (2005).

[4] E. Braaten and J. Lee, Phys. Rev. D **67**, 054007 (2003); **72**, 099901(E) (2005).

[5] K.-Y. Liu, Z.-G. He, and K.-T. Chao, Phys. Lett. B **557**, 45 (2003).

[6] J. P. Ma and Z. G. Si, Phys. Rev. D **70**, 074007 (2004).

[7] K.-Y. Liu, Z.-G. He, and K.-T. Chao, Phys. Rev. D **69**, 094027 (2004).

[8] A. E. Bondar and V. L. Chernyak, Phys. Lett. B **612**, 215 (2005).

[9] K.-Y. Liu, Z.-G. He, and K.-T. Chao, Phys. Rev. D **77**, 014002 (2008).

[10] K. Abe *et al.* (Belle Collaboration), Phys. Rev. Lett. **98**, 082001 (2007).

[11] P. Pakhlov *et al.* (Belle Collaboration), Phys. Rev. D **79**, 071101(R) (2009).

[12] P. Pakhlov *et al.* (Belle Collaboration), Phys. Rev. Lett. **100**, 202001 (2008).

[13] G. T. Bodwin, J. Lee, and E. Braaten, Phys. Rev. Lett. **90**, 162001 (2003).

[14] Y.-J. Zhang, Y.-J. Gao, and K.-T. Chao, Phys. Rev. Lett. **96**, 092001 (2006).

[15] Z.-G. He, Y. Fan, and K.-T. Chao, Phys. Rev. D **75**, 074011 (2007).

[16] G. T. Bodwin, H. S. Chung, D. Kang, J. Lee, and C. Yu, Phys. Rev. D **77**, 094017 (2008).

[17] G. T. Bodwin, J. Lee, and C. Yu, Phys. Rev. D **77**, 094018 (2008).

[18] V. V. Braguta, Phys. Rev. D **79**, 074018 (2009).

[19] H.-R. Dong, F. Feng, and Y. Jia, Phys. Rev. D **85**, 114018 (2012).

[20] N. Brambilla *et al.*, Eur. Phys. J. C **71**, 1534 (2011).

[21] N. Brambilla *et al.*, arXiv:1404.3723 (accepted by Eur. Phys. J. C).

[22] Y. Jia, Phys. Rev. D **78**, 054003 (2008).

[23] G. Bin, Y. Jia, and W. Jian-Xiong, Phys. Lett. B **670**, 350 (2009).

[24] V. V. Braguta and V. Kartvelishvili, Phys. Rev. D **81**, 014012 (2010).

[25] P. Sun, G. Hao, and Q. Cong-Feng, Phys. Lett. B **702**, 49 (2011).

[26] V. V. Braguta, A. K. Likhoded, and A. V. Luchinsky, Phys. Rev. D **72**, 094018 (2005).

[27] V. V. Braguta, A. K. Likhoded, and A. V. Luchinsky, Phys. Rev. D **80**, 094008 (2009); **85**, 119901(E) (2012).

[28] J. Zhang, H. Dong, and F. Feng, Phys. Rev. D **84**, 094031 (2011).

[29] L.-B. Chen and C.-F. Qiao, J. High Energy Phys. **11**, 168 (2012).

[30] C. P. Shen *et al.* (Belle Collaboration), Phys. Rev. D **85**, 071102(R) (2012).

[31] Y. Jia, Phys. Rev. D **76**, 074007 (2007).

[32] J. Xu, H.-R. Dong, F. Feng, Y.-J. Gao, and Y. Jia, Phys. Rev. D **87**, 094004 (2013).

[33] B. A. Irwin, B. Margolis, and H. D. Trottier, Phys. Rev. D **42**, 1577 (1990).

[34] A. Abashian *et al.* (Belle Collaboration), Nucl. Instr. and Methods Phys. Res. Sect. A **479**, 117 (2002).

[35] J. Brodzicka *et al.* (Belle Collaboration), Prog. Theor. Exp. Phys. , 04D001 (2012).

[36] S. Kurokawa and E. Kikutani, Nucl. Instr. and Methods Phys. Res. Sect. A **499**, 1 (2003), and other papers included in this volume.

[37] T. Abe *et al.* (Belle Collaboration), Prog. Theor. Exp. Phys. , 03A001 (2013), and following articles up to 03A011.

[38] D. J. Lange, Nucl. Instr. and Methods Phys. Res. Sect. A **462**, 152 (2001).

[39] K. A. Olive *et al.* (Particle Data Group), Chin. Phys. C **38**, 090001 (2014).

[40] T. Sjostrand, S. Mrenna, and P. Skands, J. High Energy Phys. **026**, 0605 (2006).

[41] A. Abashian *et al.*, Nucl. Instr. and Methods Phys. Res. Sect. A **491**, 69 (2002).

[42] K. Hanagaki *et al.*, Nucl. Instr. and Methods Phys. Res. Sect. A **485**, 490 (2002).

[43] E. Nakano, Nucl. Instr. and Methods Phys. Res. Sect. A **494**, 402 (2002).

[44] K. Wang, Y.-Q. Ma, and K.-T. Chao, Phys. Rev. D **84**, 034022 (2011), and private communication with Y. J. Zhang.

[45] A neutral cluster in the electromagnetic calorimeter is reconstructed as a photon if it does not match the extrapolated position of any charged track and its energy is greater than 40 MeV.

[46] M. Ablikim *et al.* (BESIII Collaboration), Phys. Rev. Lett. **108**, 222002 (2012).